

Electronic Supplementary Material (ESI) for Nanoscale.  
This journal is © The Royal Society of Chemistry 2015

## Supporting information

### **Sub-6 nm Monodisperse Hexagonal Core/Shell NaGdF<sub>4</sub> Nanocrystals with Enhanced Upconversion Photoluminescence**

Jing Liu<sup>a</sup>, Guanying Chen<sup>a,b\*</sup>, Shuwei Hao<sup>a</sup>, and Chunhui Yang<sup>a\*</sup>

<sup>a</sup>MIT Key Laboratory of Critical Materials Technology for New Energy Conversion and Storage,  
School of Chemistry and Chemical Engineering, Harbin Institute of Technology, Harbin, Heilongjiang  
150001, P. R. China

<sup>b</sup>Institute for Lasers, Photonics, and Biophotonics, University at Buffalo, State University of New  
York, Buffalo, NY 14260, USA

Corresponding Emails: [chenguanying@hit.edu.cn](mailto:chenguanying@hit.edu.cn); [yangchh@hit.edu.cn](mailto:yangchh@hit.edu.cn);

## Experimental Section.

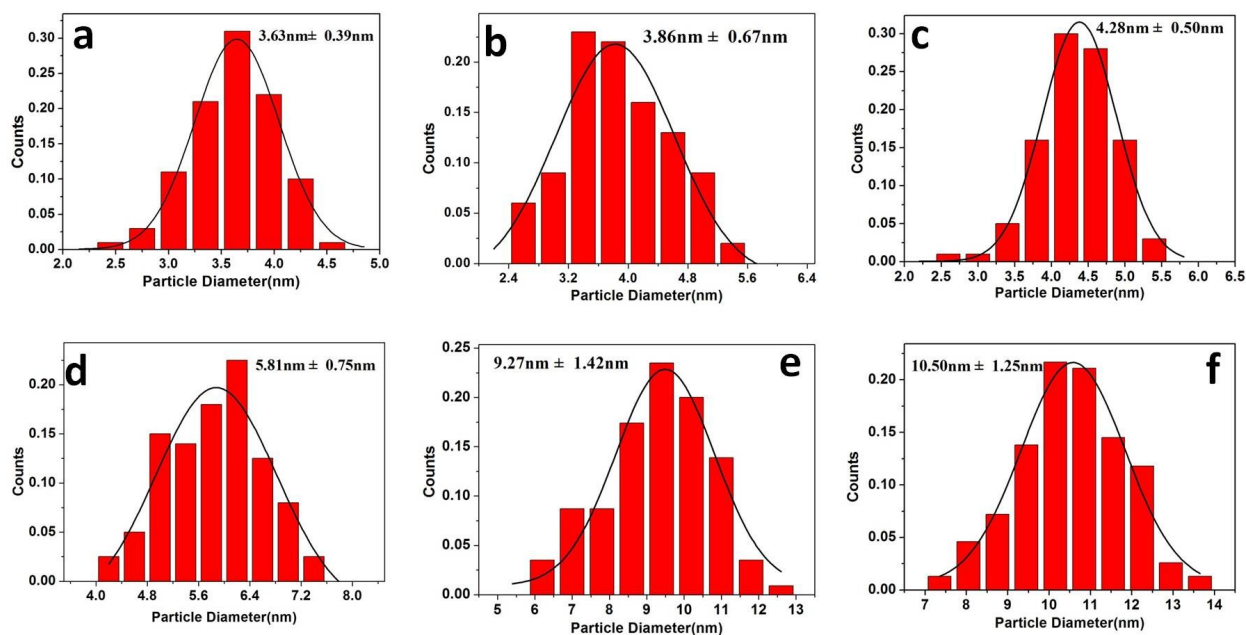


**Figure S1.** The size distribution of NaGdF<sub>4</sub>:30%Yb/ 2%Er nanocrystals prepared at different reaction temperatures: a) 240 °C; b)250 °C; c)260 °C; d)280 °C; e) 290°C; and f) 300 °C. The data of the size distributions were obtained through randomly counting of ~200 nanocrystals.

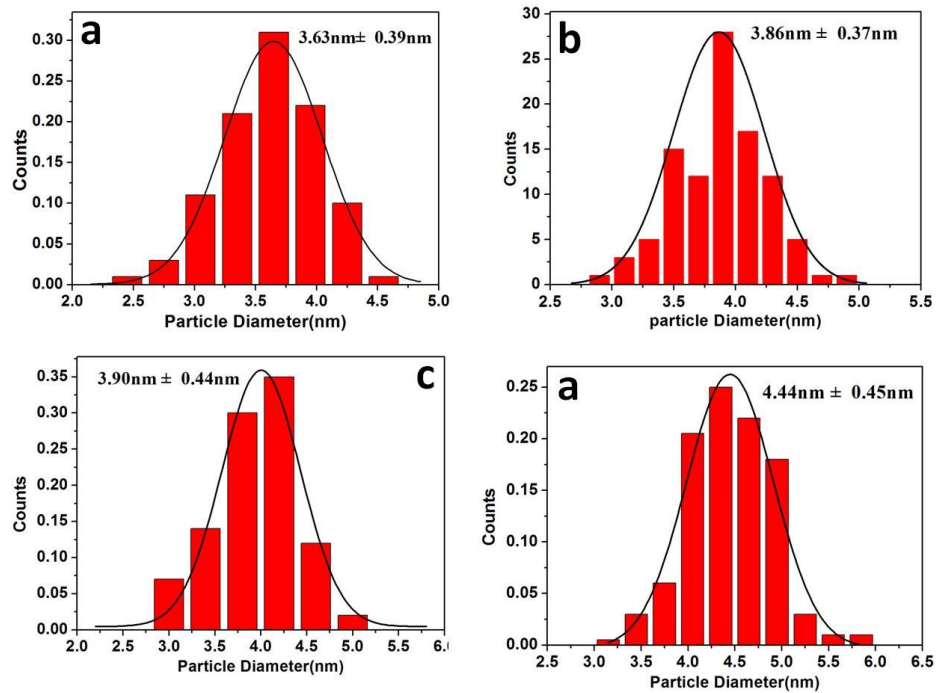


**Figure S2.** The size distribution of NaGdF<sub>4</sub>: 30%Yb/ 2%Er nanocrystals prepared at different reaction time periods: a) 20 min, b) 30 min, c) 40 min, and d) 50 min. The data of the size distributions was obtained through randomly counting ~ 200 nanocrystals.

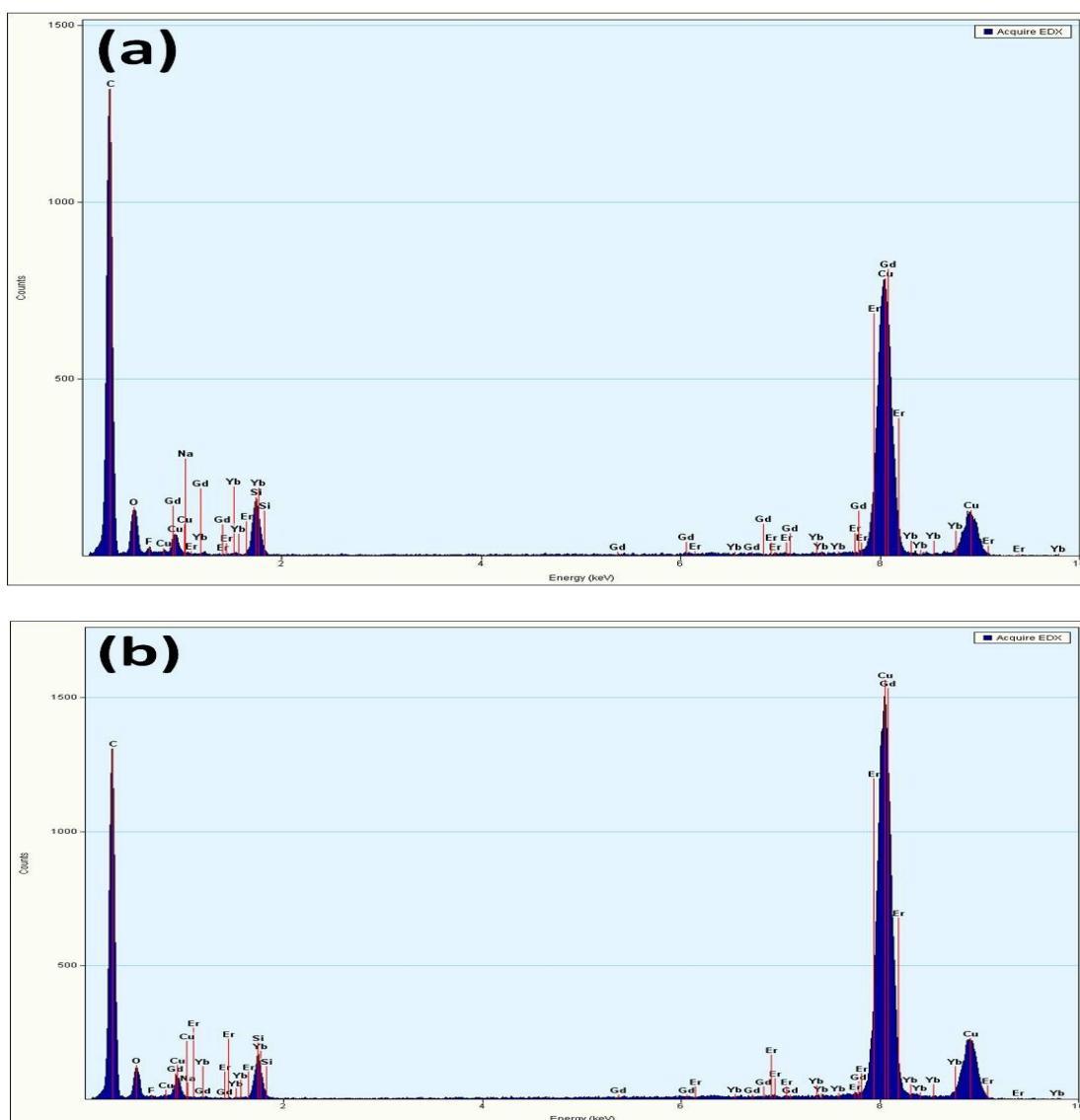


**Figure S3.** The energy-dispersive X-ray spectroscopy(EDX) of the exemplified samples of (a)NaGdF<sub>4</sub>: 30%Yb/2%Er core and NaGdF<sub>4</sub>: 30%Yb/2%Er@NaGdF<sub>4</sub> core/shell nanoparticles.

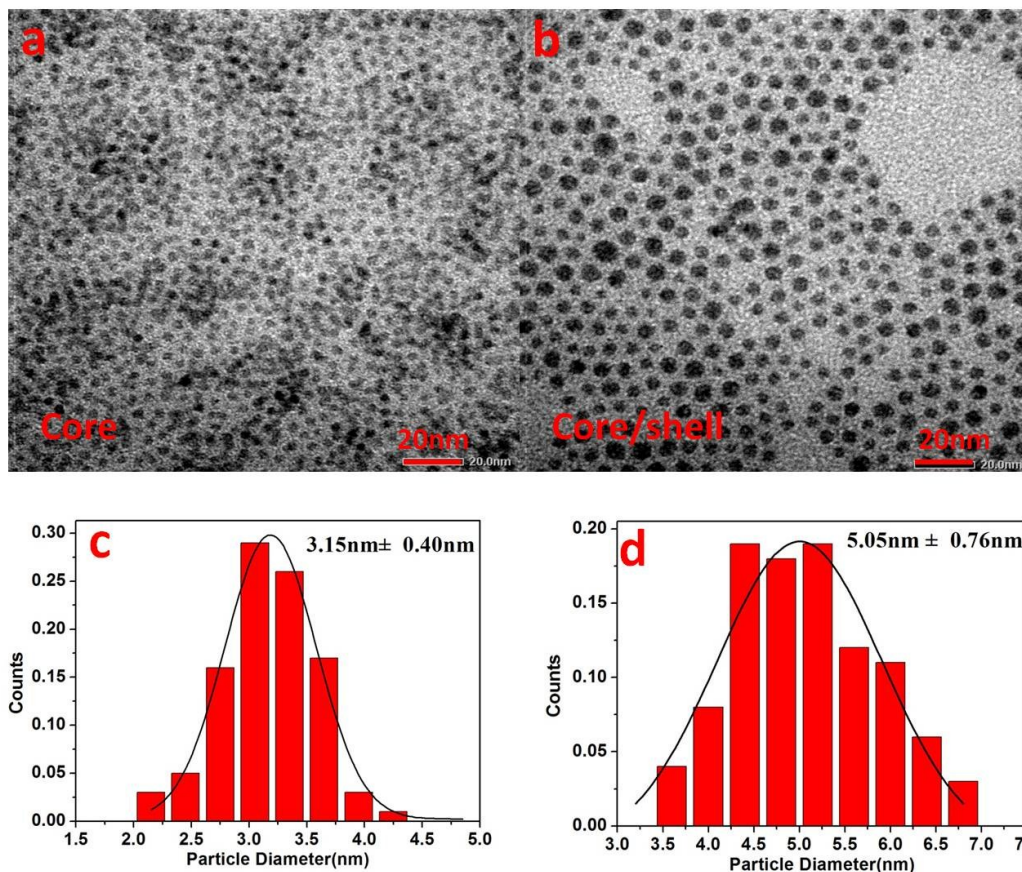


**Figure S4.** Transmission electron microscopic images of (a) the NaGdF<sub>4</sub>:20%Yb/2%Ho core nanoparticles, and (b) the NaGdF<sub>4</sub>:Yb20%/Ho2%@NaGdF<sub>4</sub> core/shell nanoparticles. The figure (c) and (d) show the size distribution histograms of the NaGdF<sub>4</sub>:20%Yb/2%Ho core and the NaGdF<sub>4</sub>:20%Yb/2%Ho@NaGdF<sub>4</sub> core/shell nanoparticles. The data of the size distribution was collected through randomly counting 200 nanocrystals in the corresponding TEM images.

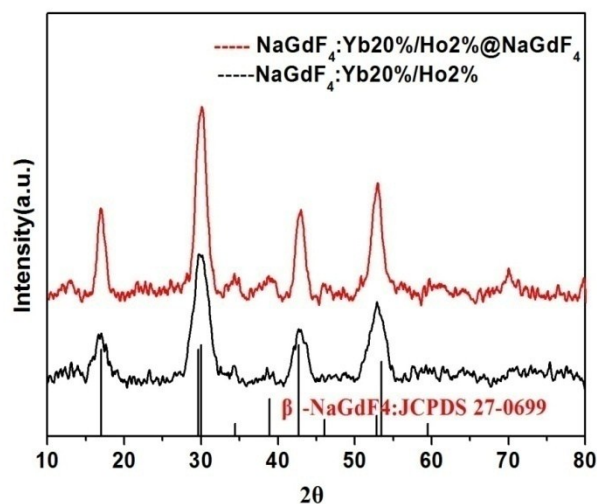


**Figure S5.** The XRD patterns of the NaGdF<sub>4</sub>:20%Yb/2%Ho<sub>core</sub> nanocrystals, and the NaGdF<sub>4</sub>:20%Yb/2%Ho@NaGdF<sub>4</sub> core/shell nanocrystals, in reference to the standard diffraction pattern of the hexagonal phase NaGdF<sub>4</sub> (JCPDS 27-0699).

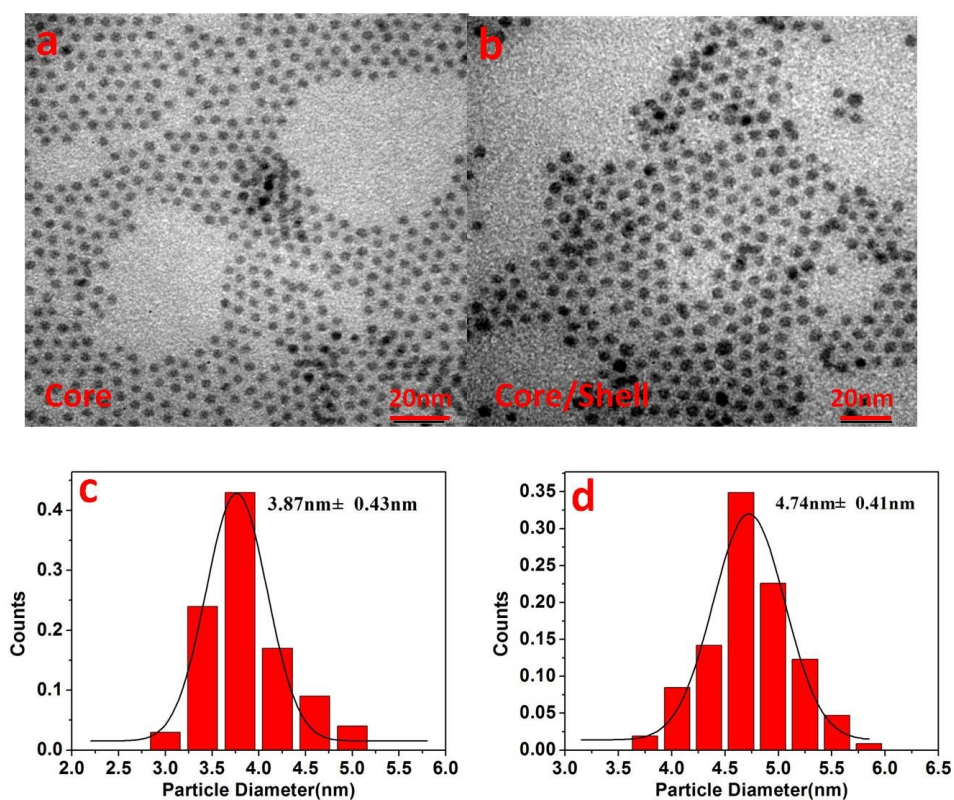


**Figure S6.** Transmission electron microscopic images of (a) the NaGdF<sub>4</sub>:30%Yb/1%Tm core nanoparticles, and (b) the NaGdF<sub>4</sub>:30%Yb/1%Tm@NaGdF<sub>4</sub> nanoparticles. The size distribution histograms of the NaGdF<sub>4</sub>:30%Yb/1%Tmcore nanoparticles as well as the NaGdF<sub>4</sub>: 30%Yb/ 1% Tm@NaGdF<sub>4</sub>core/shell nanoparticles are shown in (c) and (d), respectively. The data for the size distributions was collected through randomly counting ~200 nanocrystals in the TEM image.

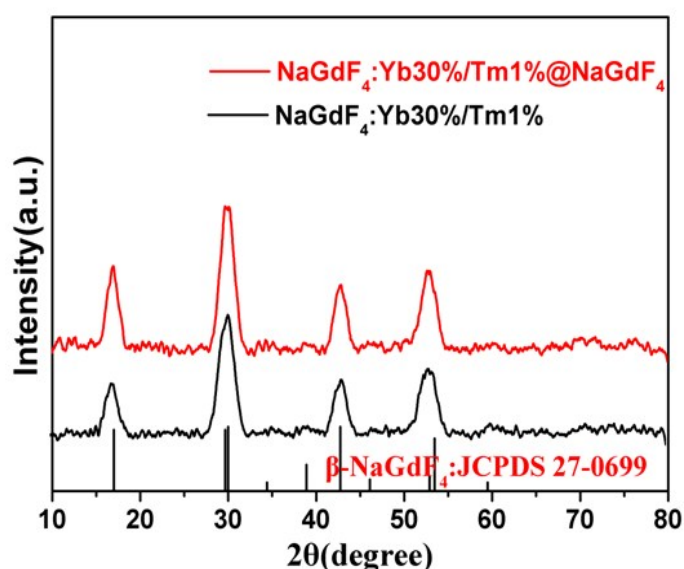


**Figure S7.** The XRD patterns of the NaGdF<sub>4</sub>: 30%Yb/ 1%Tmcore nanocrystals, and the NaGdF<sub>4</sub>: 30%Yb/ 1%Tm @ NaGdF<sub>4</sub>core/shell nanocrystals, in reference to the standard diffraction pattern of the hexagonal phase NaGdF<sub>4</sub> (JCPDS 27-0699).

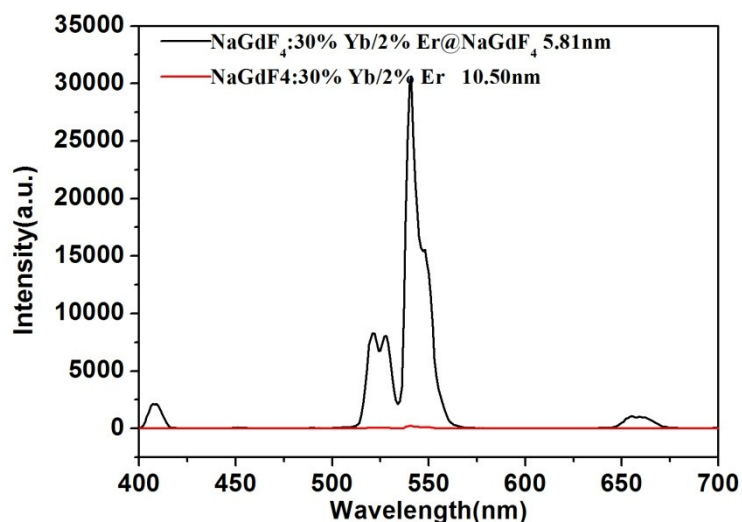


**Figure S8.** The UCPL spectra of the 10.5 nm sized NaGdF<sub>4</sub>:30%Yb/2%Er core nanocrystals and 5.81 nm sized NaGdF<sub>4</sub>:30%Yb/2%Er@NaGdF<sub>4</sub> core/shell nanocrystals (hexane dispersion). The integrated UCPL of the 5.81 nm sized core/shell nanocrystals was determined to be about 128 folds higher than that of the 10.5 nm sized core nanocrystals.

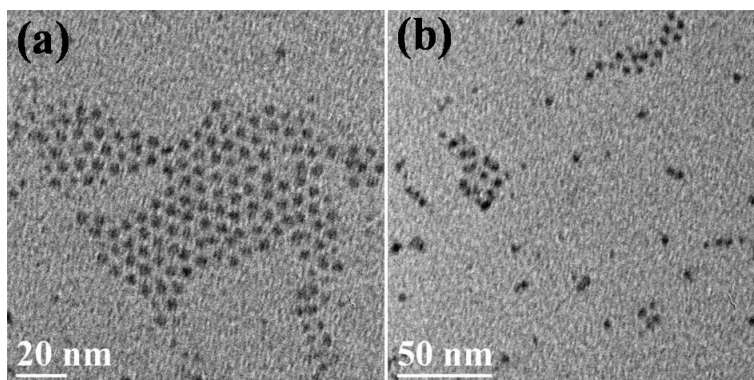


**Figure S9.** TEM images of NaGdF<sub>4</sub>:30%Yb/2%Er@NaGdF<sub>4</sub> (core/shell) upconversion nanocrystals (a) before and (b) after ligand exchange.

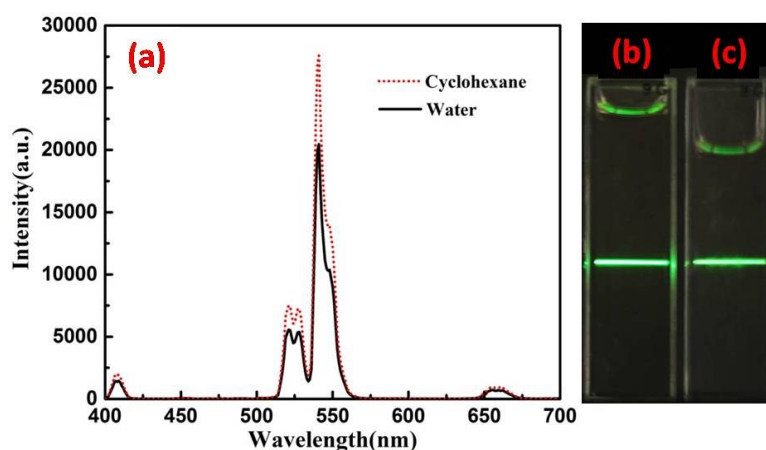


**Figure S10.** Upconversion photoluminescence (UCPL) spectra of the  $\text{NaGdF}_4:30\%\text{Yb}/2\%\text{Er}@ \text{NaGdF}_4$  core/shell nanocrystals dispersed in cyclohexane (dashed red line) and in water (solid black line). The UCPL photographic images of  $\text{NaGdF}_4:30\%\text{Yb}/2\%\text{Er}@ \text{NaGdF}_4$  nanocrystals dispersed in cyclohexane (b, prior to ligand exchange) and in water (c, after ligand exchange). Excited at 980 nm of  $70 \text{ W}/\text{cm}^2$

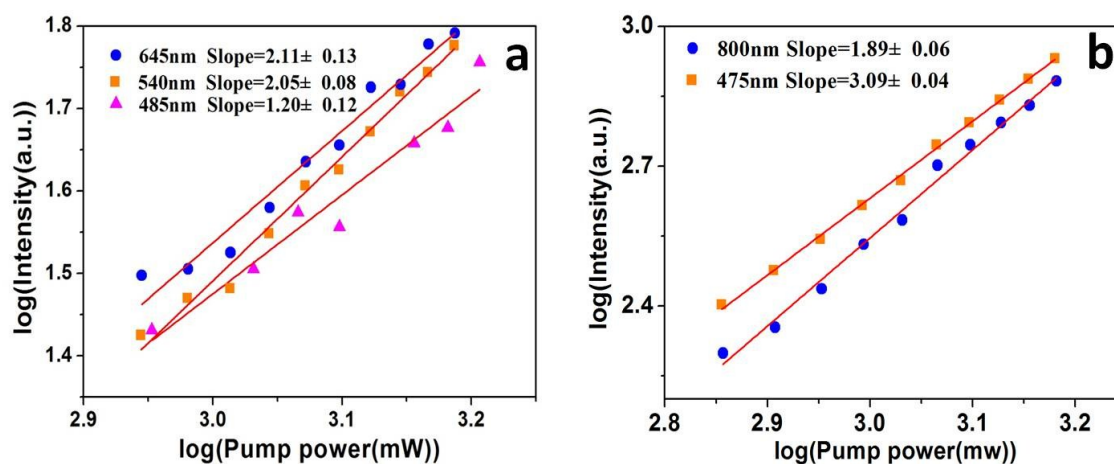


**Figure S11.** (a) A log–log plot of the intensities of various UC emission bands in Figure5a versus the excitation density for the core/shell nanocrystals of  $\text{NaGdF}_4: 20\%\text{Yb}/2\%\text{Ho}@ \text{NaGdF}_4$ . (b) A log–log plot of the intensities of various UC emission bands in Figure5b versus the excitation density for the

NaGdF<sub>4</sub>:Yb30%/Tm1%@NaGdF<sub>4</sub> core/shell nanocrystals. The slope values of the linear fits (solidline) for each UC band are presented in the inset.

As one can see in Figure S8 a, slope values of  $n = 2.11$ ,  $2.05$  and  $1.20$  were obtained for the  ${}^5F_5 \rightarrow {}^5I_8$ ,  ${}^5S_2 \rightarrow {}^5I_8$  and  ${}^5F_3 \rightarrow {}^5I_8$  transitions of Ho<sup>3+</sup>, indicating that two-photon processes are involved to populate the  ${}^5F_5$ ,  ${}^5S_2$  and  ${}^5F_3$  levels, respectively. Similarly, the slope values of  $n = 3.09$  and  $1.89$  obtained for the  ${}^1G_4 \rightarrow {}^3H_6$  and  ${}^3H_4 \rightarrow {}^3H_6$  transitions of Tm<sup>3+</sup> in Figure S8b, indicates that three- and two-photon process are involved to populate the  ${}^1G_4$  and  ${}^3H_4$  levels, respectively.

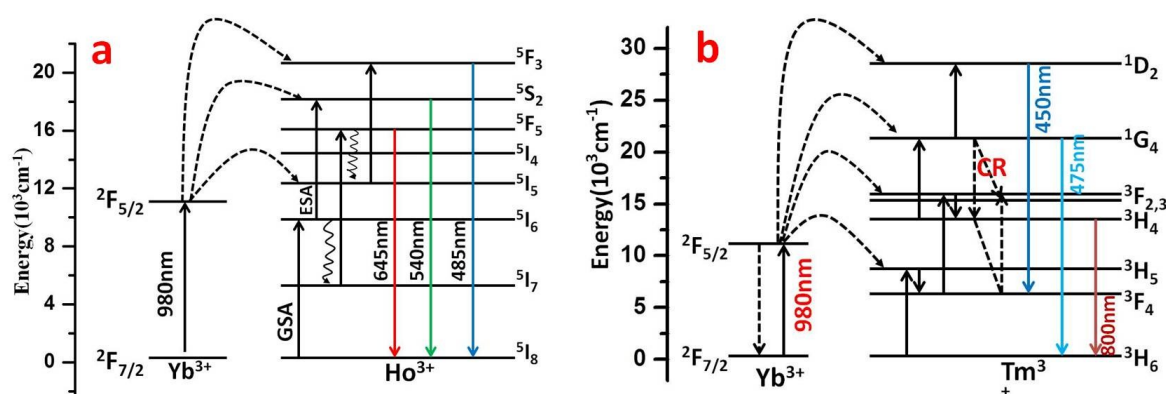


**Figure S12.** (a) Energy level diagrams of Yb and Ho ions and the proposed upconversion mechanism for the NaGdF<sub>4</sub>: 20%Yb/2%Ho@ NaGdF<sub>4</sub> nanocrystals. (b) Energy level diagrams of Yb and Tm ions and the proposed upconversion mechanism for the NaGdF<sub>4</sub>: 30%Yb/1%Tm@ NaGdF<sub>4</sub> nanocrystals.

Energy level diagram of the Ho<sup>3+</sup> and Yb<sup>3+</sup> ions as well as the UC mechanism proposed to produce the green, red and blue emission under a 980 nm laser excitation shown in Figure. S9a. Yb<sup>3+</sup> ion absorbs one laser photon and thus, is excited from the ground  ${}^2F_{7/2}$  state to the  ${}^2F_{5/2}$  state. Then, the Yb<sup>3+</sup> ion transfers its absorbed energy to the neighboring Ho<sup>3+</sup> ions to populate the  ${}^5I_6$  excited level. The energy difference between the two levels was abridged by the vibration energy of the host lattice. The

population in the  $^5I_6$  level can be promoted to the  $^5S_2$  levels either by excited state absorption (ESA) or by energy transfer (ET) from another excited  $Yb^{3+}$  ion. When the  $^5S_2$  level is populated, the excited electron can release its energy by emitting green emissions. The red emission at 645 nm can be produced by irradiative decay to the ground state from the  $^5F_5$  state, which can be populated by two possible ways. (i) Excited from the intermediate  $^5I_7$  using the energy transfer process of  $^2F_{5/2}(Yb^{3+}) + ^5I_7(Ho^{3+}) \rightarrow ^2F_{7/2}(Yb^{3+}) + ^5F_5(Ho^{3+})$ , (ii) multiphonon-assisted relaxations from the  $^5S_2$  excited levels to the  $^5F_5$  level. Some ions at the  $^5I_5$  level can be promoted to the  $^5F_3$  level, from which weak emission at 485 nm is produced. The green emission at 540nm is produced by radiative decay to the ground state from the  $^5S_2$  state.

In analogy, for the Yb-Tm doped core/shell nanocrystals, the  $Yb^{3+}$  ions also firstly absorb laser photons at  $\sim 980$  nm, and are excited from the ground state  $^2F_{5/2}$  to the  $^2F_{7/2}$  state. Then, the  $Yb^{3+}$  ions in their excited states successively transfer the absorbed energy to the  $Tm^{3+}$  ion, and promote it from the ground state to the  $^3H_5$  (first step),  $^3F_{2,3}$  (second step),  $^1G_4$  (third step),  $^1D_2$  (fourth step) states, respectively. Multi-phonons from the lattice are involved to assist the energy transfer from  $Yb^{3+}$  to  $Tm^{3+}$  ions. Nonradiative relaxations from the  $^3F_{2,3}$  state can populate the  $^3H_4$  state, from which the near infrared (NIR) emission at 800 nm is produced. It should be noted that the cross-relaxation process of  $^1G_4 + ^3F_4 \rightarrow ^3H_4 + ^3F_2$  can contribute to populate the  $^3H_4$  state. The blue emission at 475 nm stems from radiative relaxations from the  $^1G_4$  state to the ground  $^3H_6$  state.